

Two-Channel Kondo Effect in Carbon Nanotube Quantum Dot

Igor Kuzmenko, Tetyana Kuzmenko, Yshai Avishai

Ben Gurion University of the Negev, P.O.B. 653, Beer Sheva, Israel
igorkuz@post.bgu.ac.il

Abstract

We consider Kondo tunneling through a junction as shown in Fig. 1(a): It is composed of two semi-infinite carbon nanotubes (CNT) that serve as left and right leads (CNTL and CNTR, respectively) attached on both sides of a short CNT quantum dot with an atom A having an s-wave valence electron of spin $S_A=1/2$ implanted on its axis (CNTQDA). The two wave numbers (valleys) \mathbf{K} and \mathbf{K}' (located on the two corners of the hexagonal Brillouin zone of the CNT) serve as two symmetry protected flavor quantum numbers $\xi=\mathbf{K}, \mathbf{K}'$. The CNTQDA is gated such that its (neutral) ground state consists of the caged atom with spin $\pm 1/2$ while its lowest excited (charged) states are singlet and triplet states, see Fig. 1(b). The energies of the singlet and triplet states satisfy inequality $\varepsilon_S > \varepsilon_T$. The Anderson model hybridizes lead and dot electrons with the same flavor and spin projection, and the Schrieffer-Wolf transformation, while mixing spin projections does not mix flavors, thereby realizing a two-channel Kondo physics.

Employing the poor man's scaling technique to the Kondo Hamiltonian, it is shown that when the ultraviolet cut off energy $\varepsilon_T - \varepsilon_F$ exceeds the Fermi energy ε_F (measured from the bottom of the conduction band), there are two different regimes of renormalization depending either the effective bandwidth D is above or below its critical value $D_1 = \varepsilon_F$, as shown in Fig. 2.

The RG flow pattern of the effective couplings k and j (corresponding to spin-independent potential scattering and spin-flipping exchange interaction) on the effective bandwidth D and the Fermi energy ε_F is shown in Fig. 3 for the energy of the triplet state $\varepsilon_T = 18$ meV. The flow of $k(D)$ as a function of D is shown in Fig. 3(a) and that of $j(D)$ is shown in Fig. 3(b) for different values of ε_F . The behavior of the curves (1), (2) and (3) [$\varepsilon_F \leq 1.7$ meV] reveals a remarkable scenario of different RG domains: Within the interval $D_0 > D > D_1$, the effective coupling $j(D)$ increases above j^* (where $j^* = 1/2$ is the two-channel fixed point value for j), and then within the interval $D < D_1$, $j(D)$ decreases approaching j^* . This behavior is unexpected, since in the standard two-channel Kondo model, the exchange coupling changes *monotonically* with D approaching j^* for $D \rightarrow 0$. The non-monotonic behavior is caused by the crossover from the single-channel RG regime for $D > D_1$ to the two-channel RG regime for $D < D_1$.

The Kondo temperature T_K is shown in Fig. 4(a) as a function of ε_T and ε_F . It is seen that T_K changes in between 0.5 K and 5 K for reasonable parameter values.

The conductance G as function of the temperature T is shown in Fig. 4(b) for $\varepsilon_T = 18$ meV and different values of ε_F . Note the non-monotonic behavior of the conductance for $\varepsilon_F \leq 1.7$ meV [curves (1)-(3)]. This exotic behavior is caused by the non-monotony of $j(T)$ [see Fig. 3(b)]. In the standard 2CKE, $G(T)$ is monotonic, depending on the bare value j_0 of j . If $j_0 < j^*$, ($j_0 > j^*$), the conductance increases (decreases) monotonically with reducing T . Non-monotony of $G(T)$ exposed here is the result of the crossover between different RG scaling regimes. One of the paradigms of the two-channel Kondo effect is that the physics related to over-screening is exposed only in the strong coupling regime, where $T < T_K$. In this work we have demonstrated that the some physical phenomena related to over-screening can be exposed also in the weak coupling regime, where $T \gg T_K$.

References

- [1] P. Nozières and A. Blandin, J. Physique, **41** (1980) 193.
- [2] I. Kuzmenko, T. Kuzmenko and Y. Avishai, submitted to Phys. Rev. B; arXiv:1408.4935.

Figures

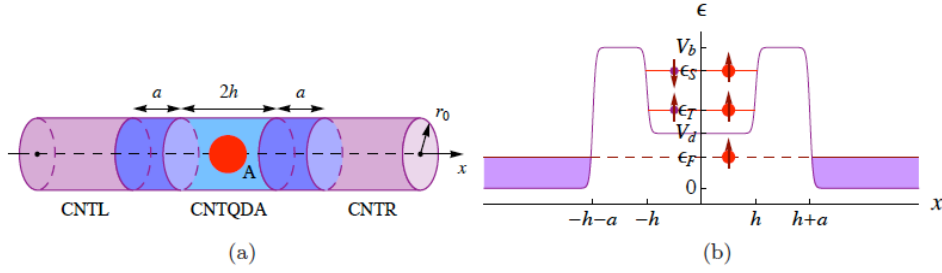


Figure 1: CNTL-CNTQDA-CNTR junction. (a) Schematic geometry of the junction including semi-infinite left and right leads, separated from a quantum dot of length $2h$ (that hosts a spin 1/2 atom A) by two barriers of width a . (b) Low energy levels of the quantum dot with (from below) the caged atom, followed by triplet and singlet atom-electron states.

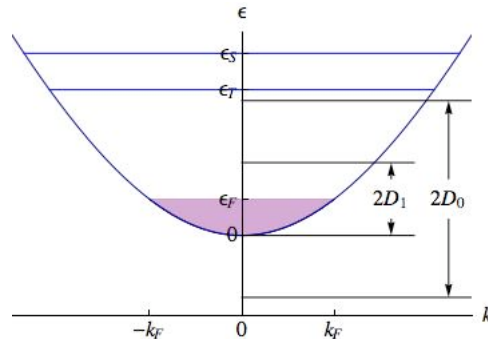


Figure 2: Two different intervals of the effective bandwidth D , where different RG regimes are expected.

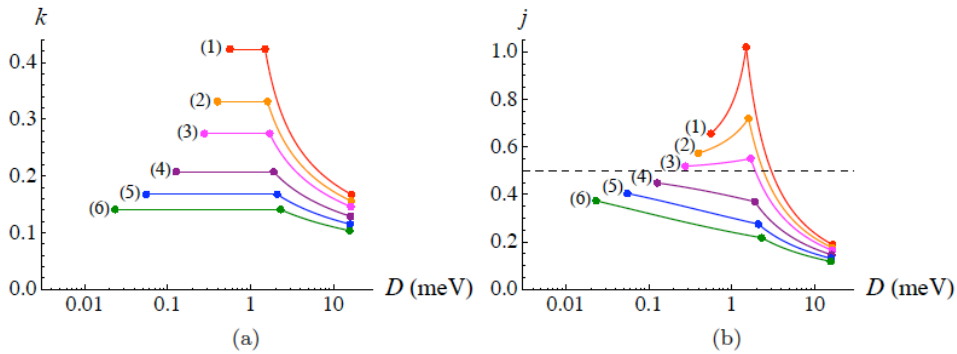


Figure 3: (a) k and (b) j as functions of D for $\epsilon_T=18$ meV and different values ϵ_F . Here $\epsilon_S-\epsilon_T=120$ meV and curves (1)-(6) correspond to $\epsilon_F=1.5, 1.6, 1.7, 1.9, 2.1$ and 2.3 meV, respectively.

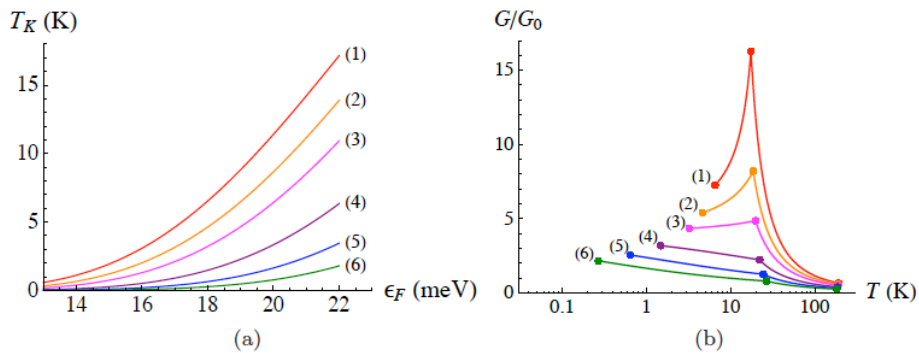


Figure 4: (a) T_K as a function of ϵ_T and different values of ϵ_F . (b) G as function of T for $\epsilon_T=18$ meV and different values of ϵ_F . For both panels, curves (1)-(6) correspond to $\epsilon_F=1.5, 1.6, 1.7, 1.9, 2.1$ and 2.3 meV, respectively. In panel (b), the dots from right to left correspond to D_0, D_1 and T_K , separating the RG regimes from one another.